Shear Wave Velocity Profiling & Rock Mass Characterization at Pavagadh Hill Using the Multichannel Analysis of Surface Waves (MASW)

Mayurkumar Aherwal[1,*], Manish Shah[2] and Usha Patel[1]

[1]Applied Mechanics Department, L.D. College of Engineering, Ahmedabad, Gujarat, India

[2]Civil Engineering Department, Government Engineering College, Bharuch, Gujarat, India

Abstract: Multichannel Analysis of Surface Waves (MASW) is a geophysical method used for subsurface characterization by measuring the variation of shear-wave velocity (Vs) with depth and evaluating the stiffness properties of near-surface materials. The prime focus of this study is MASW testing was carried out at multiple locations situated at different elevations of Pavagadh Hill to characterize subsurface rock mass conditions and to understand the variation of engineering parameters along the hill slope. Conventional borehole-based seismic testing methods such as cross-hole and downhole testing are expensive, intrusive and spatially limited in heterogeneous geological conditions. Surface wave based geophysical techniques have therefore emerged as efficient and non-destructive alternatives for continuous subsurface characterization. Among these techniques, the Multichannel Analysis of Surface Waves (MASW) method has become one of the most accepted approaches for estimating shear-wave velocity profiles using the dispersive characteristics of Rayleigh waves propagating through layered media. The obtained Vs profiles were used to evaluate variation in subsurface stiffness and rock mass conditions with depth at different elevations. Further, Vs_{30} values were calculated for selected locations and the sites were classified according to NEHRP site classification criteria. Based on the estimated shear wave velocity important engineering parameters such as shear modulus (G), rock mass deformation modulus (Em), Geological Strength Index (GSI), Uniaxial Compressive Strength (UCS) and bearing capacity were evaluated. The results obtained from this study provide valuable input for safe foundation design, slope stability assessment and infrastructure development at Pavagadh Hill.

Keyword: Pavagadh Hill, Multichannel Analysis of Surface Waves, Shear Wave Velocity, Rock Mass Characterization, Geological Strength Index, Foundation Engineering.

INTRODUCTION

Subsurface rock mass characterization plays an essential role in civil engineering projects such as foundations, slope stability assessment, tunnelling, seismic site evaluation and infrastructure development in hilly terrains. Reliable identification of engineering bedrock depth and evaluation of rock mass stiffness are critical for safe and economical design of structures constructed over rock formations. Conventional rock investigation techniques such as borehole drilling, core logging and laboratory testing provide accurate information but are often expensive, time-consuming and limited to discrete locations.

In recent years, non-destructive geophysical methods have gained significant importance for rapid and continuous subsurface profiling of rock formations. Among these techniques, the Multichannel Analysis of Surface Waves (MASW) method has emerged as a reliable and efficient approach for determining shear wave velocity (Vs) profiles of subsurface rock layers. Since shear wave velocity is directly related to the elastic properties and stiffness of rock masses, MASW surveys provide valuable information for identifying weathered zones, fractured rock layers and competent engineering bedrock.

The MASW technique was first introduced by Park *et al*. (1999), who demonstrated its capability to obtain near-surface shear-wave velocity profiles from Rayleigh-wave dispersion data. Subsequently, Xia *et al*. (1999) further validated the methodology for subsurface characterization. Miller *et al*. (2000) applied MASW in engineering and environmental investigations, highlighting its effectiveness in delineating subsurface stratigraphy. Later studies by Kanli *et al*. (2006) employed MASW for seismic microzonation and site characterization, while Cox *et al*. (2011) examined the reliability and uncertainty associated with MASW-derived velocity profiles. Foti *et al*. (2014) provided a comprehensive overview of surface-wave methods, emphasizing the importance of MASW in geotechnical and earthquake engineering applications.

The MASW technique utilizes dispersive characteristics of Rayleigh surface waves recorded through multiple geophones arranged along a linear profile. Analysis of surface wave dispersion curves allows estimation of shear wave velocity variation with depth, which can be used to evaluate dynamic elastic parameters such as Shear modulus and Young's modulus of rock masses. These parameters are essential for geotechnical design and rock engineering applications.

*Address correspondence to this author at the Applied Mechanics Department, L.D. College of Engineering, Ahmedabad, Gujarat, India;
E-mail: mayuraherwal@gmail.com

Received on 13-05-2026 Accepted on 10-07-2026 Published on 23-07-2026

E-ISSN: 3083-3590/26

PAVAGADH HILL

Pavagadh Hill is located in the Panchmahal district of Gujarat in western India, approximately 50 km east of Vadodara and about 68 km south of Godhra. The hill rises prominently from the surrounding plain and forms a distinct volcanic outlier of the Deccan Trap province with an elevation of about 829 m above mean sea level. At the base of the hill lies the historic city of Champaner and together they form the internationally recognized Champaner–Pavagadh Archaeological Park, which was declared a UNESCO World Heritage Site in 2004 due to its archaeological, cultural and historical importance.

Figure 1: Pavagadh Hill.

The region is also well known for the Mahakali Temple one of the important Shaktipeeth pilgrimage sites in India that attracts thousands of visitors daily. Because of its geological prominence, historical importance and ongoing infrastructure development activities associated with tourism and pilgrimage, subsurface characterization of the Pavagadh hill region is essential for safe engineering planning and slope stability evaluation.

Pavagadh Hill represents a prominent volcanic outlier located within the northern extent of the Deccan Volcanic Province in western India. The hill forms part of the Champaner volcanic complex and preserves a well-defined volcanic stratigraphic succession associated with Late Cretaceous to Early Paleogene magmatic activity, approximately 65–69 million years ago.

Geologically, the Pavagadh Hill sequence consists predominantly of basaltic lava flows representing multiple eruptive units such as picritic and mugearitic basalt formed during different phases of volcanic activity. These lava flows are separated by flow contacts, cooling joints and discontinuity surfaces that significantly influence the structural and mechanical behaviour of the rock mass. Such structural features play an important role in controlling subsurface stiffness variation and engineering bedrock conditions within the volcanic terrain.

Rhyolitic volcanic formations are also exposed within the Pavagadh hill complex and represent acidic volcanic activity associated with the Champaner volcanic centre. These rhyolitic units occur within the volcanic succession and contribute to the overall lithological framework of the study area. The presence of such volcanic units reflects the complex eruptive history of the region and plays an important role in defining subsurface rock mass conditions relevant to engineering investigations.

Structurally, the volcanic sequence in the study area is affected by columnar jointing, fractures, flow boundaries and weathering zones formed due to cooling processes and subsequent tectonic adjustments. Near-surface formations are generally characterized by weathered volcanic rock layers, while moderately weathered and fresh rock formations occur at greater depths. The thickness of weathered zones varies spatially depending on slope geometry, drainage characteristics and fracture density within the rock mass.

From an engineering perspective, the heterogeneous volcanic stratigraphy and variable weathering profile of the Pavagadh hill region strongly influence subsurface stiffness distribution and engineering bedrock depth. Therefore, identification of competent rock layers within this volcanic terrain is essential for geotechnical investigations and infrastructure planning. In this context, the Multi-Channel Analysis of Surface Waves (MASW) technique provides an effective non-destructive approach for determining shear wave velocity variation with depth and identify subsurface within the study area.

FIELD TESTING LOCATIONS

In the study seven locations were selected at different elevations on Pavagadh Hill for conducting MASW field testing. The selected test points include Location 1 (770 m; 22°27′58.13″N, 73°30′54.48″E), Location 2 (735 m; 22°28′01.04″N, 73°30′44.67″E), Location 3 (690 m; 22°28′07.89″N, 73°30′56.96″E), Location 4 (545 m; 22°27′40.74″N, 73°31′42.30″E), Location 5 (505 m; 22°27′43.66″N, 73°31′34.56″E), Location 6 (485 m; 22°27′50.68″N, 73°31′27.29″E), and Location 7 (475 m; 22°27′56.59″N, 73°31′23.37″E).

These locations were carefully selected at different elevations along Pavagadh Hill to obtain representative shear-wave velocity (Vs) profiles and to evaluate the

Figure 2: Field Testing Locations.

Table 1: **Details of Study Area**

Study Area	Elevation	Source Offset	No. of Profile
Location 1	770 m	15 m, 25 m, 30 m	3
Location 2	735 m	20 m, 25 m, 30 m	3
Location 3	690 m	15 m, 20 m, 25 m, 30 m	4
Location 4	545 m	20 m, 25 m	2
Location 5	505 m	20 m, 25 m, 30 m	3
Location 6	485 m	15 m, 20 m, 25 m, 30 m	4
Location 7	475 m	15 m, 20 m, 30 m	3

variation in subsurface rock mass parameters across the study area.

FIELD TESTING PROCEDURE

The MASW field testing procedure at Pavagadh Hill was carried out by deploying a linear array of equally spaced vertical geophones along the selected survey line at each test location. A metal base plate was placed at a fixed offset from the first geophone and seismic energy was generated using repeated hammer impacts to produce surface waves. The generated wave signals were recorded simultaneously by a multichannel seismic data acquisition system and monitored in the field to ensure proper coupling and minimal noise. Multiple recordings were taken at each location to improve signal quality and the collected data were stored for further dispersion analysis and inversion to obtain shear-wave velocity profiles.

Typical Acquisition Parameters Included

- Seismograph: ECHO 24
- Number of geophones: 24
- Geophone spacing: 4 m
- Geophone frequency: 4.5 Hz
- Total spread length: 96 m
- Source offset: 15 m, 20 m, 25 m, 30 m
- Sampling interval: 1 ms
- Record length: 2 sec
- Acquisition mode: Active MASW linear array configuration
- Source type: 10 kg hammer with base plate

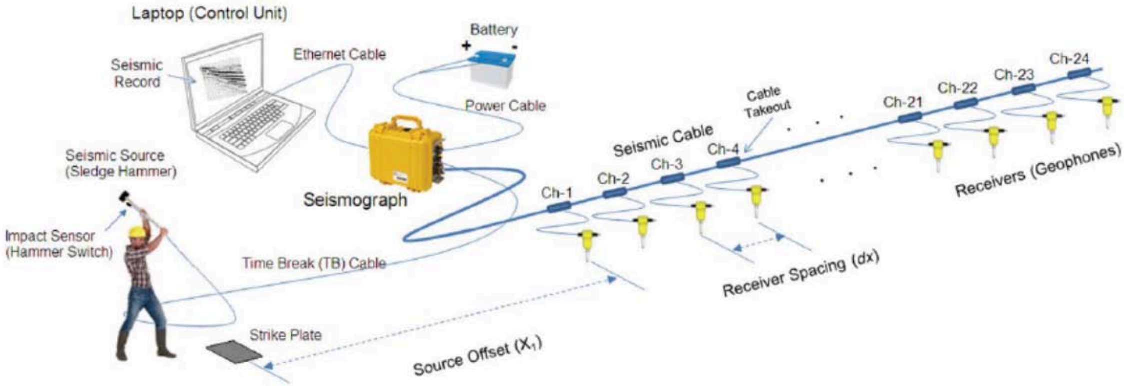

Figure 3: Field Testing Arrangement.

- Number of stacks: 3–5 hammer blows per shot point

DISPERSION & INVERSION ANALYSIS

In this research work, the processing of MASW seismic records was carried out in two main stages: dispersion analysis and inversion analysis. These steps were performed using GeoGiga Surface Plus software to determine the shear-wave velocity (Vs) profile of the subsurface layers. In the dispersion analysis stage, the recorded seismic data were first imported into the software and the survey geometry, including geophone spacing and source position was defined. The software then transformed the seismic records from the time–distance domain into the frequency–phase velocity domain to generate dispersion images. From these images the fundamental-mode dispersion curve was identified and extracted for further processing. In the inversion stage, the extracted dispersion curve was used to create an initial layered velocity model which was iteratively refined by matching theoretical dispersion curves with the measured curve until an acceptable fit was obtained. The final output of this process provided the variation of shear-wave velocity with depth which was used for interpretation of subsurface conditions.

At each test location multiple seismic records were acquired using different source offsets during the MASW survey to improve the reliability and depth coverage of the subsurface investigation. The shear-wave velocity (Vs) profiles obtained from individual source offsets were processed separately through dispersion analysis and inversion procedures. To obtain a representative subsurface profile for each test point, the Vs values corresponding to different offsets were combined and an average shear-wave velocity profile was calculated at each location.

SITE CLASSIFICATION

Site classification is the process of categorizing ground conditions based on subsurface stiffness and seismic response characteristics. In geotechnical and earthquake engineering studies site classification is commonly determined using the Shear-wave velocity of the upper 30 m of soil or rock, known as $\mathbf{Vs_{30}}$. This parameter helps evaluate how ground conditions influence seismic wave amplification and structural performance during earthquakes.

$\mathbf{Vs_{30}}$ is calculated using the following equation given in NEHRP guideline:

$$V_{S30} = \frac{\sum_{i=1}^{N_L} t_i}{\sum_{i=1}^{N_L} \left(\frac{t_i}{V_{Si}}\right)}$$

Where,

N_L = Number of layers within the depth of influence

t_i = Thickness (m) of layer i within the depth of influence

V_{Si} = Shear wave velocity (m/s) of layer i

Table 2: Site Classification as Per NEHRP

Site Class	Description	Shear-wave Velocity Definition
A	Hard rock	Vs_{30} > 1,500 m/s
B	Rock	760 m/s < Vs_{30} <1,500 m/s
C	Cer dense soil and soft rock	360 m/s < Vs_{30} < 760 m/s
D	Stiff soil	180 m/s < Vs_{30} < 360 m/s
E	Soil with soft clay	Vs_{30} < 180 m/s

SHEAR MODULUS (G)

The Shear modulus is a measure of a material's resistance to deformation when subjected to shear stress. It represents the ratio of shear stress to the corresponding shear strain within the elastic limit of the material. A higher shear modulus indicates greater stiffness and stronger resistance to shape change under lateral forces.

Shear Modulus is calculated using the following equation:

$G = \rho\, Vs^2$

Where,

G = Shear Modulus (MPa)

ρ = Density of the Material (Rock)

Vs = Shear Wave Velocity (m/s)

Density assumption in this research work given below:

Vs < 360 m/s ρ = 2200 kg/m^3

Vs 360-760 m/s ρ = 2400 kg/m^3

Vs 760-1500 m/s ρ = 2600 kg/m^3

Vs >1500 m/s ρ = 2800 kg/m^3

YOUNG'S MODULUS (E)

The Young's modulus also known as the modulus of deformation, is a fundamental mechanical property that describes the stiffness of a material when subjected to axial loading such as tension or compression. It represents the ratio of normal stress to the corresponding normal strain within the elastic limit of the material. A higher value of Young's modulus indicates that the material is stiffer and undergoes less deformation under applied load, whereas a lower value indicates more flexibility.

Young's modulus is calculated using the following equation:

$E = 2\, G\, (1+v)$

Where,

$E = E_m$ = Young's modulus (MPa)

G= Shear modulus (MPa)

ν= Poisson's ratio (Consider 0.25)

GEOLOGICAL STRENGTH INDEX (GSI)

The Geological Strength Index (GSI) is a rock mass classification system used to estimate the strength and deformation properties of jointed rock masses. It is based on the structure of the rock mass (degree of fracturing and blockiness) and the surface condition of discontinuities such as roughness, weathering and infilling. GSI values typically range from 10 to 100, where lower values indicate poor-quality, highly fractured rock and higher values indicate strong, intact rock masses.

The Geological Strength Index (GSI) to estimate the deformation modulus of a rock mass using the empirical relationship proposed by Evert Hoek and Erik Diederichs (2006) given below:

$$E_m = 100000 * \frac{\left(1 - \frac{D}{2}\right)}{\left(1 + e^{\frac{75 + 25D - GSI}{11}}\right)}$$

Rearranging the equation for GSI

$$GSI = 75 + 25D - 11 \ln\left\{\left(\frac{100000 * \left(1 - \frac{D}{2}\right)}{E_m}\right) - 1\right\}$$

Where,

GSI = Geological Strength Index

E_m = Rock Mass Deformation Modulus / Young's modulus (MPa)

D= Disturbance Factor (0 for undisturbed rock mass)

ln = Natural Logarithm

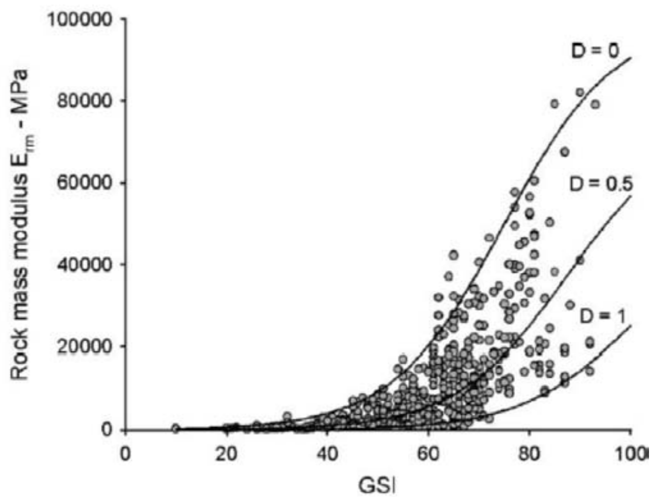

Figure 5: Relation Between GSI & Rock Mass Deformation Modulus.

UNIAXIAL COMPRESSIVE STRENGTH (UCS)

The Uniaxial compressive strength (UCS) of rock is a fundamental engineering parameter that represents the maximum compressive stress a rock specimen can withstand under axial loading without lateral confinement. It is used to evaluate the strength and

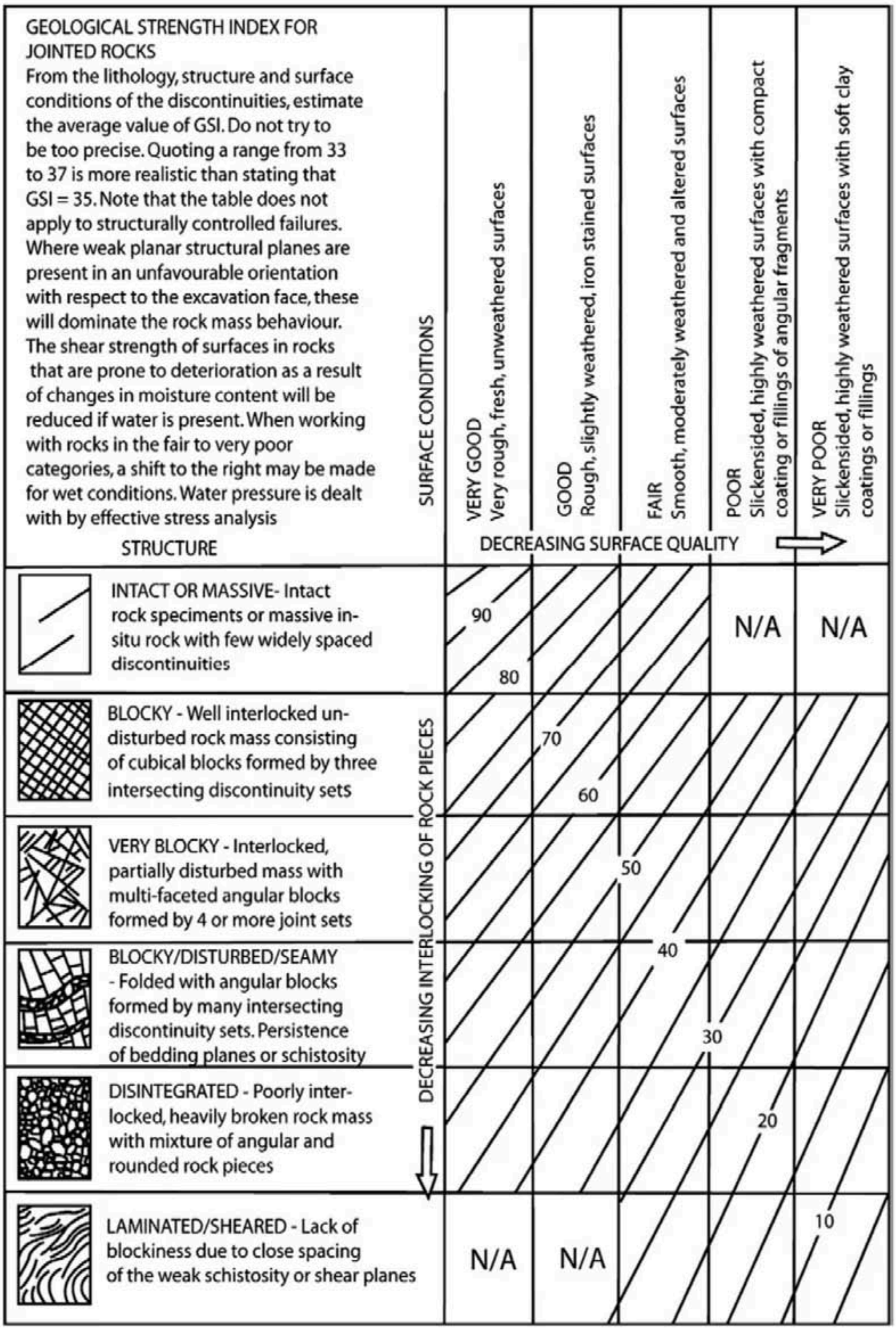

Figure 6: Basic GSI chart (Hoek and Marinos, 2000).

load-bearing capacity of intact rock material and plays an important role in rock mass classification, slope stability assessment, tunnel design and foundation engineering.

The Uniaxial compressive strength (UCS) of rock can also be estimated using the empirical relationship proposed by E. Hoek, C. Carranza-Torres and B. Corkum (2002) given below:

$$\mathrm{E}_m = 1000\left(1 - \frac{\mathrm{D}}{2}\right) * \sqrt{\left(\frac{\sigma_{ci}}{100}\right)} * 10^{\frac{(\mathrm{GSI}-10)}{40}}$$

Rearranging the equation for UCS

$$\sigma_{ci} = 100 * \left\{\frac{\frac{\mathrm{E}_m}{1000}}{\left(1 - \frac{\mathrm{D}}{2}\right) * 10^{\frac{(\mathrm{GSI}-10)}{40}}}\right\}^2$$

Where,

σ_{ci} = Uniaxial Compressive Strength of Intact Rock (MPa)

E_m = Rock Mass Deformation Modulus / Young Modulus (MPa)

GSI = Geological Strength Index

D = disturbance factor (0 for undisturbed rock mass)

BEARING CAPACITY

The Bearing capacity of soil or rock is the maximum load that the ground can safely support without experiencing shear failure or excessive settlement. It is an important parameter in foundation engineering because it helps determine the size and type of foundation required to safely transfer structural loads to the ground. Higher bearing capacity values indicate stronger and more stable ground conditions suitable for supporting heavier structures, whereas lower values require special design considerations to ensure safety and stability.

As per the IS 12070: 1987 bearing capacity equation given below:

$$q_a = \sigma_{ci} * N_q$$

Where,

q_a = Allowable Bearing Capacity of Rock (MPa)

σ_{ci} = Uniaxial Compressive Strength of Intact Rock (MPa)

N_q = Bearing Capacity Factor (Consider 0.1)

Typical Values of N_q

Highly weathered / fractured rock / Spacing of Discontinuities 30-100 cm = **0.10**

Moderately weathered rock / Spacing of Discontinuities 100-300 cm = **0.25**

Slightly weathered / hard rock / Spacing of Discontinuities >300 cm = **0.4**

Net Bearing Capacity

$$q_n = \frac{q_a}{FOS}$$

Where,

q_n = Net Bearing Capacity of Rock (MPa)

q_a = Allowable Bearing Capacity of Rock (MPa)

FOS = Factor of Safety = 3

REPRESENTATIVE PHOTOGRAPHS OF MASW FIELD TESTING

Figure 7: MASW Survey Equipment and Accessories Used for Field Testing.

Figure 8: Preparation of MASW Survey Line at the Test Location.

Figure 9: Deployment of Seismic Cable.

Figure 10: Installation and Connection of Geophones Along the Survey Line.

Figure 13: Portable Data Acquisition System with Power Supply and Control Unit.

Figure 11: Geophone Array Arrangement for Surface Wave Data Acquisition.

Figure 14: Real-Time Monitoring and Recording of MASW Data in the Field.

Figure 12: Generation of Seismic Waves Using a Sledgehammer Source.

Figure 15: Display of Recorded Seismic Waveforms During Data Acquisition.

RESULTS

Location 1

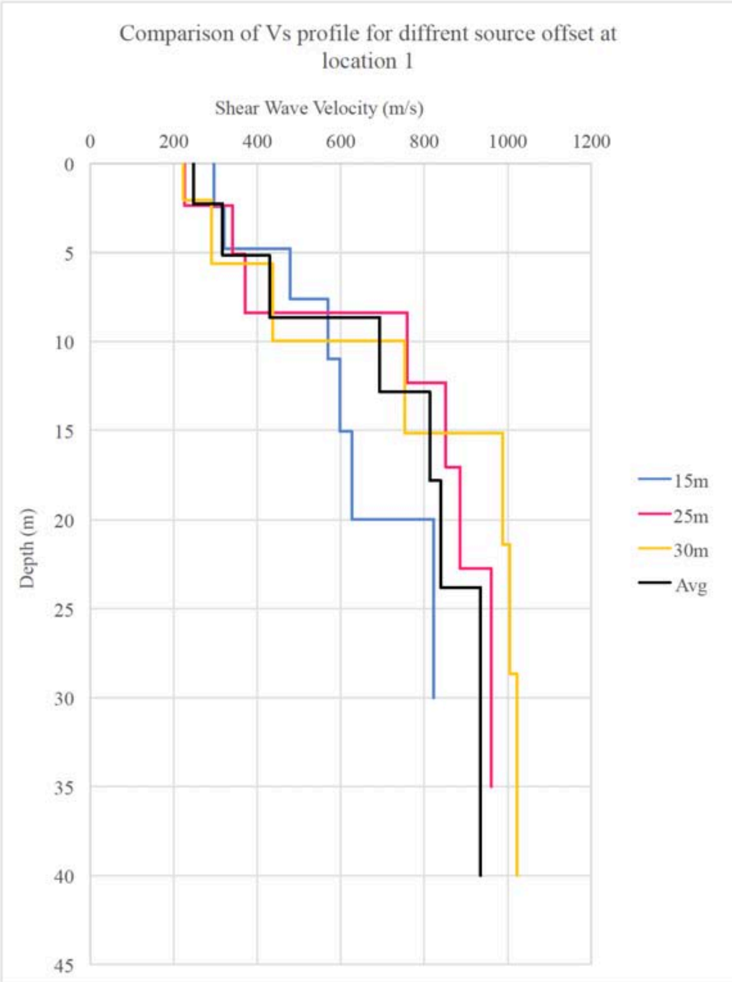

Figure 16: Vs Profiles at Location 1.

Table 3: Vs Profiles Obtained Using Different Source Offsets at Location 1

15m Source Offset		25m Source Offset		30m Source Offset	
Depth	Vs	Depth	Vs	Depth	Vs
2.43	296	2.35	225	2.05	223
4.78	321	5.09	340	5.65	291
7.61	479	8.38	370	9.98	438
11	569	12.33	759	15.16	753
15.07	599	17.07	852	21.39	988
19.96	627	22.76	886	28.66	1005
30	823	35	961	40	1022

Table 4: Rock Mass Parameters for Average Vs Profile at Location 1

Depth (m)	Vs (m/s)	Density (kg/m^3)	G (MPa)	E_m (MPa)	GSI	UCS (MPa)	q_a (MPa)	q_n (MPa)	q_n (t/m^2)
2.28	248	2200	135.31	338.27	12	8.62	0.86	0.29	29.32
5.17	317	2200	221.54	553.85	18	12.35	1.23	0.41	41.98
8.66	429	2400	441.70	1104.25	26	20.34	2.03	0.68	69.15
12.83	694	2400	1154.82	2887.04	36	40.23	4.02	1.34	136.77
17.84	813	2600	1718.52	4296.30	41	52.86	5.29	1.76	179.72
23.79	839	2600	1831.65	4579.12	42	55.18	5.52	1.84	187.62
40	935	2600	2274.61	5686.51	44	63.74	6.37	2.12	216.70

Location 2

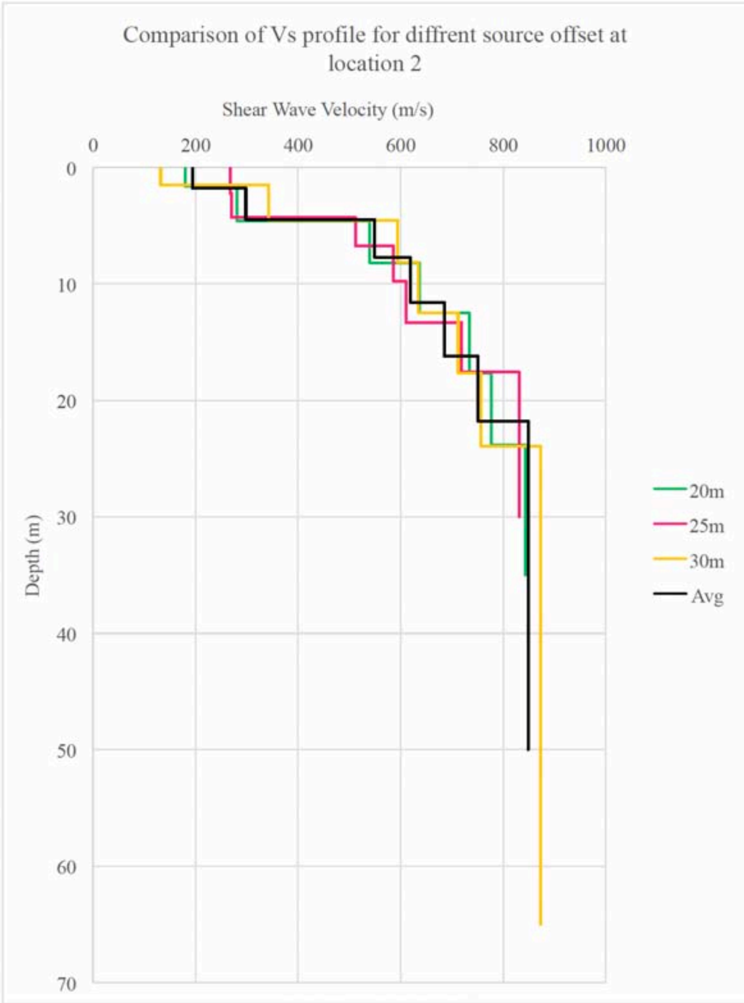

Figure 17: Vs Profiles at Location 2.

Table 5*:* **Vs Profiles Obtained Using Different Source Offsets at Location 2**

20m Source Offset		25m Source Offset		30m Source Offset	
Depth	**Vs**	**Depth**	**Vs**	**Depth**	**Vs**
1.63	180	2.23	268	1.53	160
4.62	281	4.3	270	4.54	343
8.2	540	6.77	512	8.15	594
12.5	636	9.74	585	12.49	635
17.65	734	13.31	610	17.7	712
23.84	777	17.58	719	23.95	757
35	843	30	831	65	873

Table 6*:* **Rock Mass Parameters for Average Vs Profile at Location 2**

Depth (m)	Vs (m/s)	Density (kg/m^3)	G (MPa)	E_m (MPa)	GSI	UCS (MPa)	q_a (MPa)	q_n (MPa)	q_n (t/m^2)
1.80	193	2200	81.95	204.87	7	5.98	0.60	0.20	20.33
4.49	298	2200	195.37	488.42	17	11.27	1.13	0.38	38.31
7.71	549	2400	722.48	1806.21	31	28.92	2.89	0.96	98.32
11.58	619	2400	918.60	2296.49	34	34.27	3.43	1.14	116.52
16.22	685	2400	1127.24	2818.09	36	39.55	3.96	1.32	134.49
21.79	751	2400	1353.60	3384.01	38	44.90	4.49	1.50	152.67
50.00	849	2600	1874.08	4685.21	42	56.04	5.60	1.87	190.53

Location 3

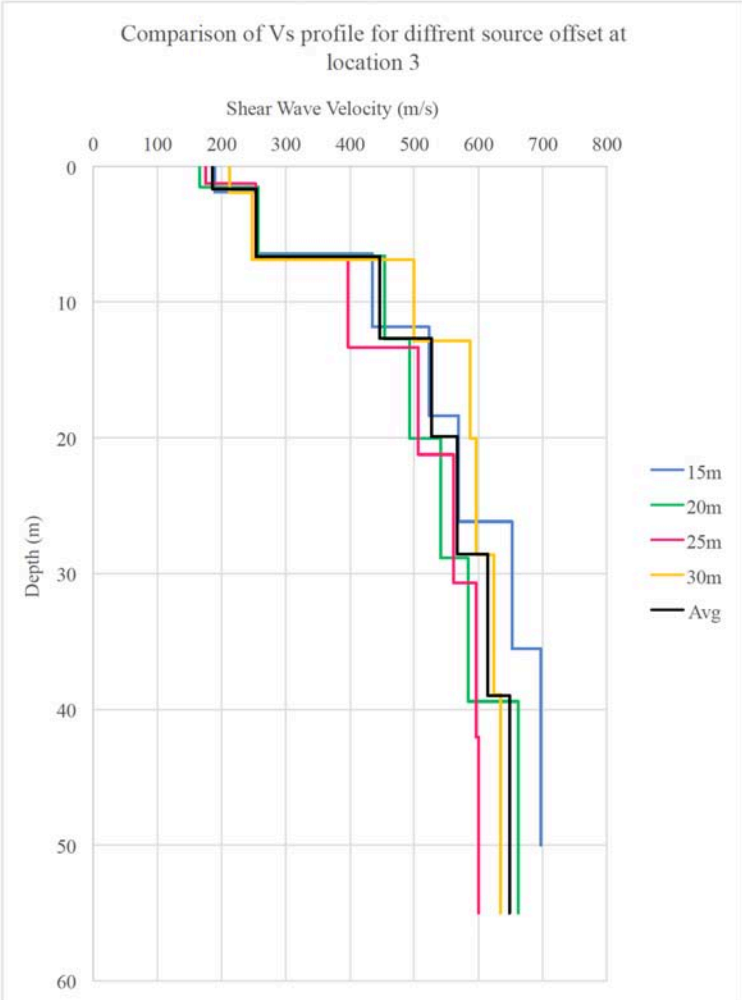

Figure 18: Vs Profiles at Location 3.

Table 7: **Vs Profiles Obtained Using Different Source Offsets at Location 3**

15m Source Offset		20m Source Offset		25m Source Offset		30m Source Offset	
Depth	Vs	Depth	Vs	Depth	Vs	Depth	Vs
1.88	189	1.51	166	1.26	175	1.93	212
6.41	257	6.6	257	6.74	253	6.89	248
11.83	435	12.71	454	13.32	397	12.86	499
18.34	523	20.05	493	21.21	506	20.01	587
26.15	569	28.85	541	30.68	561	28.6	596
35.53	652	39.42	584	42.05	596	38.9	624
50	697	55	662	55	600	55	634

Table 8: **Rock Mass Parameters for Average Vs Profile at Location 3**

Depth (m)	Vs (m/s)	Density (kg/m^3)	G (MPa)	E_m (MPa)	GSI	UCS (MPa)	q_a (MPa)	q_n (MPa)	q_n (t/m^2)
1.65	186	2200	75.70	189.26	6	5.64	0.56	0.19	19.18
6.66	254	2200	141.66	354.14	13	8.92	0.89	0.30	30.31
12.68	446	2400	477.93	1194.83	26	21.53	2.15	0.72	73.19
19.90	527	2400	667.18	1667.96	30	27.33	2.73	0.91	92.91
28.57	567	2400	770.89	1927.23	32	30.28	3.03	1.01	102.95
38.98	614	2400	904.79	2261.98	34	33.91	3.39	1.13	115.29
55.00	648	2400	1008.55	2521.37	35	36.60	3.66	1.22	124.43

Location 4

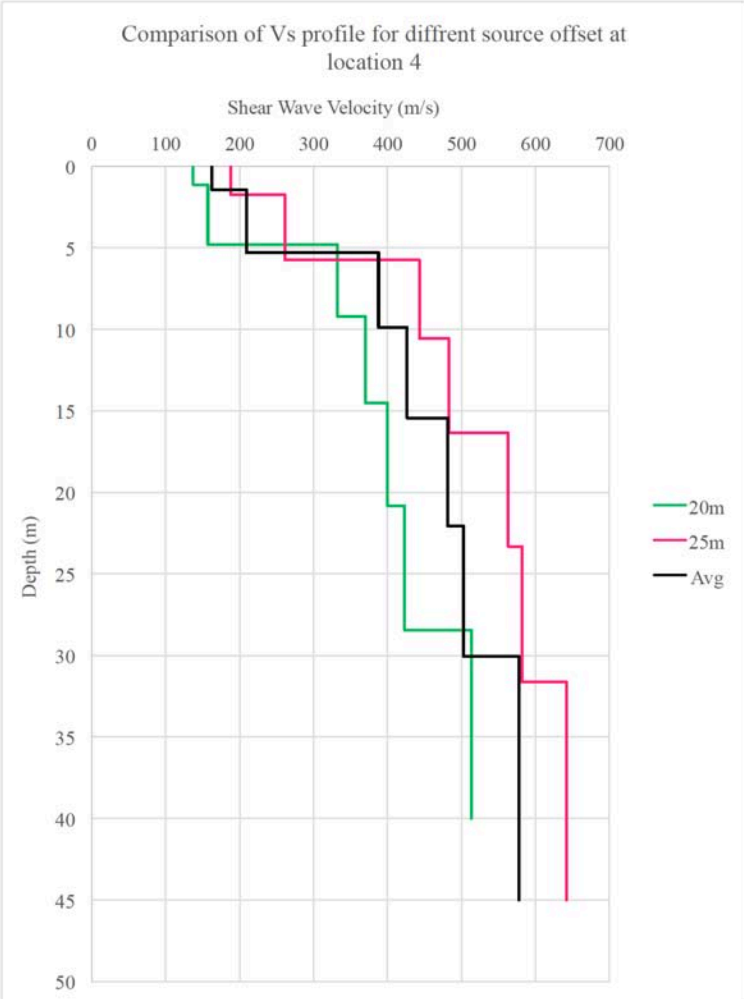

Figure 19: Vs Profiles at Location 4.

Table 9: Vs Profiles Obtained Using Different Source Offsets at Location 4

20m Source Offset		25m Source Offset	
Depth	Vs	Depth	Vs
1.14	137	1.74	188
4.81	157	5.76	261
9.21	332	10.58	443
14.5	370	16.37	483
20.84	400	23.31	563
28.45	423	31.64	582
40	513	45	642

Table 10*:* Rock Mass Parameters for Average Vs Profile at Location 4

Depth (m)	Vs (m/s)	Density (kg/m^3)	G (MPa)	E_m (MPa)	GSI	UCS (MPa)	q_a (MPa)	q_n (MPa)	q_n (t/m^2)
1.44	163	2200	58.09	145.23	3	4.65	0.46	0.15	15.81
5.29	209	2200	96.10	240.25	9	6.72	0.67	0.22	22.84
9.90	388	2400	360.38	900.94	23	17.56	1.76	0.59	59.72
15.44	427	2400	436.57	1091.41	25	20.17	2.02	0.67	68.57
22.08	482	2400	556.42	1391.05	28	24.00	2.40	0.80	81.62
30.05	503	2400	606.02	1515.04	29	25.52	2.55	0.85	86.75
45.00	578	2400	800.42	2001.04	32	31.10	3.11	1.04	105.73

Location 5

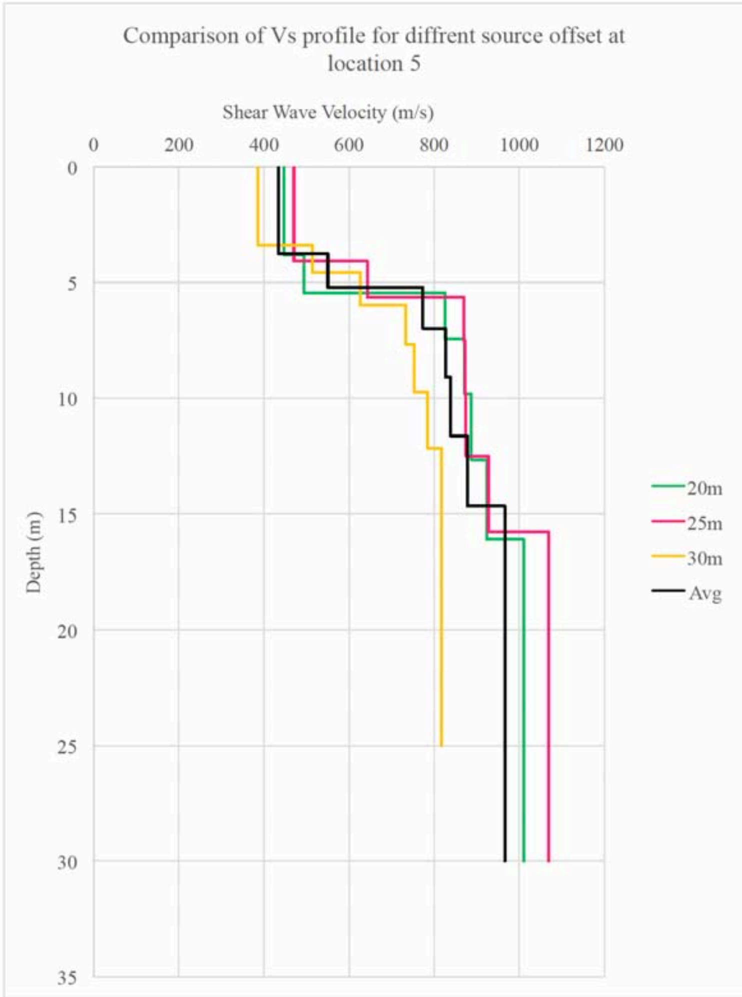

Figure 20: Vs Profiles at Location 5.

Table 11: Vs Profiles Obtained Using Different Source Offsets at Location 5

20m Source Offset		25m Source Offset		30m Source Offset	
Depth	**Vs**	**Depth**	**Vs**	**Depth**	**Vs**
3.81	447	4.07	471	3.39	386
5.46	495	5.64	643	4.57	514
7.44	826	7.52	870	5.99	626
9.82	872	9.79	873	7.69	734
12.66	887	12.5	875	9.73	753
16.08	924	15.76	928	12.17	785
30	1011	30	1070	25	818

Table 12*:* Rock Mass Parameters for Average Vs Profile at Location 5

Depth (m)	Vs (m/s)	Density (kg/m^3)	G (MPa)	E_m (MPa)	GSI	UCS (MPa)	q_a (MPa)	q_n (MPa)	q_n (t/m^2)
3.76	435	2400	453.44	1133.61	26	20.73	2.07	0.69	70.47
5.22	551	2400	727.76	1819.40	31	29.07	2.91	0.97	98.83
6.98	774	2600	1557.60	3893.99	40	49.44	4.94	1.65	168.10
9.10	826	2600	1775.35	4438.37	41	54.03	5.40	1.80	183.71
11.63	838	2600	1827.29	4568.22	42	55.09	5.51	1.84	187.32
14.67	879	2600	2008.87	5022.17	43	58.70	5.87	1.96	199.59
30.00	966	2600	2427.88	6069.70	45	66.51	6.65	2.22	226.15

Location 6

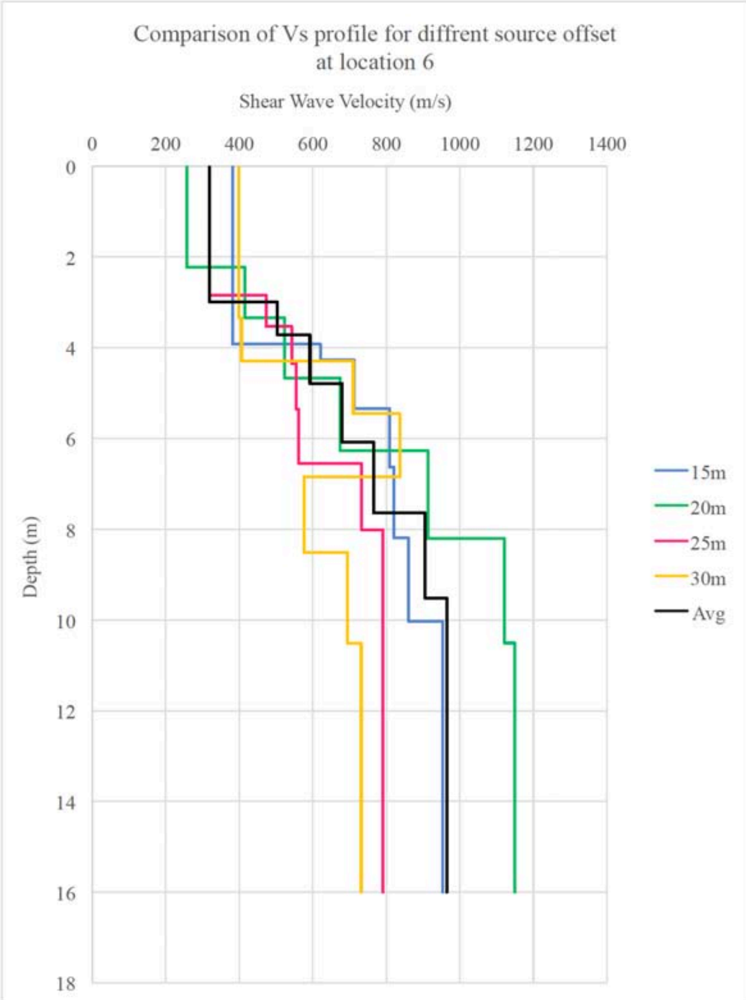

Figure 21: Vs Profiles at Location 6.

Table 13: Vs Profiles Obtained Using Different Source Offsets at Location 6

15m Source Offset		20m Source Offset		25m Source Offset		30m Source Offset	
Depth	**Vs**	**Depth**	**Vs**	**Depth**	**Vs**	**Depth**	**Vs**
3.93	381	2.23	257	2.84	320	3.34	399
4.28	622	3.34	415	3.53	473	4.3	406
5.35	712	4.67	523	4.36	543	5.46	710
6.64	809	6.27	675	5.36	556	6.85	837
8.18	821	8.2	914	6.56	562	8.51	576
10.02	861	10.5	1121	8.01	733	10.51	695
16	954	16	1150	16	791	16	732

Table 14: Rock Mass Parameters for Average Vs Profile at Location 6

Depth (m)	Vs (m/s)	Density (kg/m^3)	G (MPa)	E_m (MPa)	GSI	UCS (MPa)	q_a (MPa)	q_n (MPa)	q_n (t/m^2)
3.00	319	2200	224.34	560.86	18	12.46	1.25	0.42	42.36
3.72	503	2400	608.03	1520.07	29	25.58	2.56	0.85	86.96
4.79	593	2400	843.01	2107.52	33	32.26	3.23	1.08	109.68
6.09	680	2400	1109.76	2774.40	36	39.13	3.91	1.30	133.03
7.65	766	2600	1524.24	3810.60	39	48.72	4.87	1.62	165.64
9.51	905	2600	2129.47	5323.66	43	61.02	6.10	2.03	207.48
16.00	965	2600	2421.19	6052.96	45	66.40	6.64	2.21	225.74

Location 7

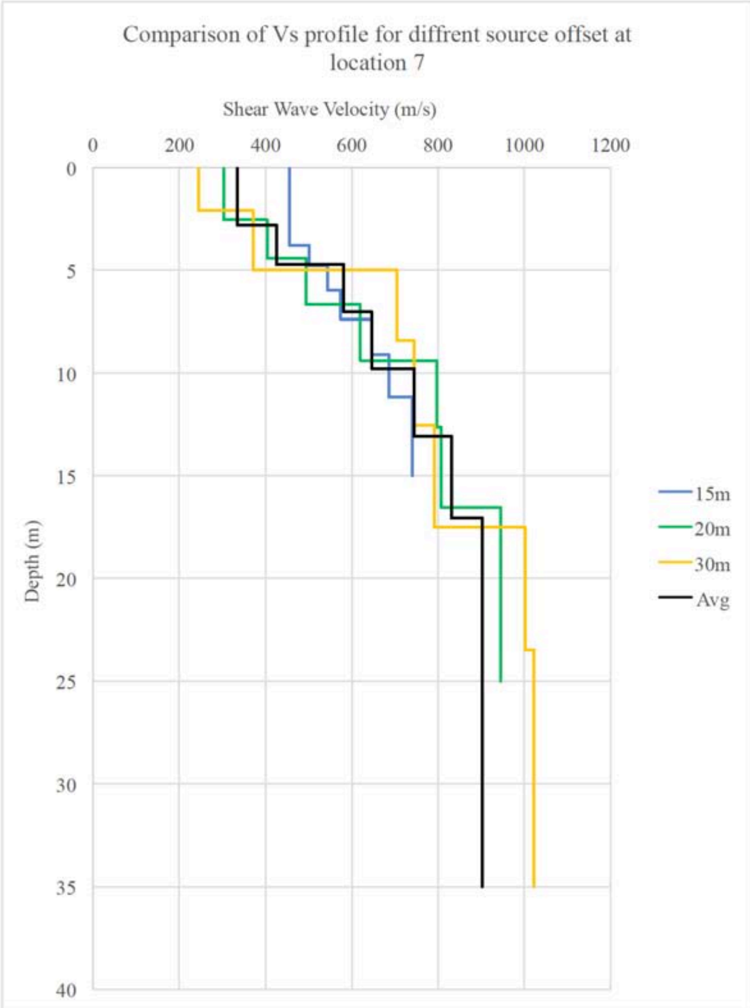

Figure 22: Vs Profiles at Location 7.

Table 15: Vs Profiles Obtained Using Different Source Offsets at Location 7

15m Source Offset		20m Source Offset		30m Source Offset	
Depth	Vs	Depth	Vs	Depth	Vs
3.78	456	2.53	303	2.09	244
4.77	501	4.41	404	4.97	371
5.96	544	6.67	494	8.41	704
7.39	574	9.38	620	12.55	744
9.1	647	12.63	797	17.51	791
11.16	686	16.53	807	23.47	1002
15	741	25	945	35	1023

Table 16: Rock Mass Parameters for Average Vs Profile at Location 7

Depth (m)	Vs (m/s)	Density (kg/m^3)	G (MPa)	E_m (MPa)	GSI	UCS (MPa)	q_a (MPa)	q_n (MPa)	q_n (t/m^2)
2.80	334	2200	245.91	614.78	19	13.32	1.33	0.44	45.28
4.72	425	2400	434.18	1085.45	25	20.09	2.01	0.67	68.30
7.01	581	2400	809.22	2023.04	32	31.34	3.13	1.04	106.55
9.77	646	2400	1001.56	2503.90	35	36.42	3.64	1.21	123.82
13.08	745	2400	1332.06	3330.15	38	44.41	4.44	1.48	151.00
17.05	832	2600	1798.34	4495.85	41	54.50	5.45	1.82	185.32
35.00	903	2600	2120.06	5300.16	43	60.84	6.08	2.03	206.87

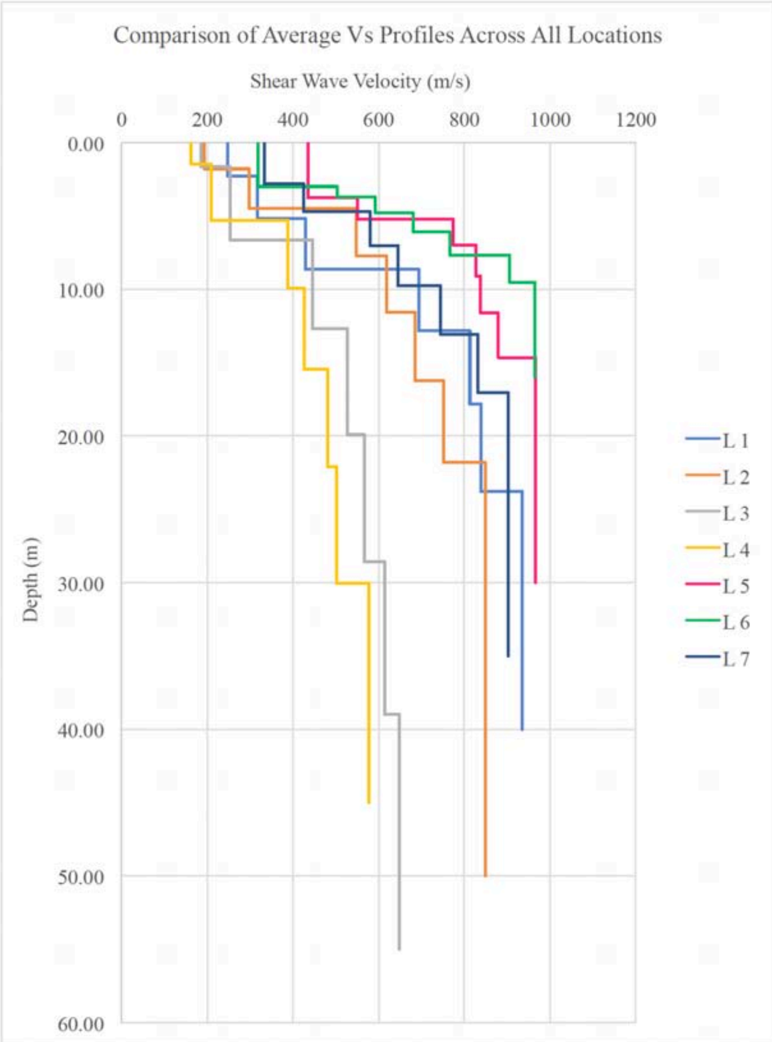

Figure 23: Comparation of Average Vs Profiles Across All Locations.

Table 17: Vs30 & Site Classification

Location	Vs_{30} (m/s)	Site Classification
Location 1	573	Class C
Location 2	552	Class C
Location 3	409	Class C
Location 4	368	Class C
Location 5	780	Class B
Location 6	Not to Classify	
Location 7	672	Class C

CONCLUSION

In this study, the Multichannel Analysis of Surface Waves (MASW) method was successfully applied at different elevations of Pavagadh Hill to evaluate subsurface conditions and characterize the engineering parameters of the rock mass. Shear-wave velocity (Vs) profiles were obtained at each location using different source offsets and representative average Vs profiles were developed to understand the overall variation of subsurface stiffness with depth across the study area.

The comparison of shear-wave velocity (Vs) profiles obtained at different source offsets and test points indicates that the average Vs profile at each location provides the most reliable representation of subsurface conditions. The averaged profile minimizes local variations caused by acquisition geometry, surface irregularities and signal noise, and therefore better reflects the overall stiffness characteristics of the rock mass. Hence, the average Vs profile across all locations is considered the most suitable and representative profile for interpretation of site subsurface conditions.

Based on the calculated Vs30 values all locations were classified according to the National Earthquake Hazards Reduction Program (NEHRP) site classification system. The calculated engineering parameters show noticeable variation between locations due to differences in subsurface weathering conditions and rock mass quality. However, overall results indicate that the subsurface formations possess moderate to high stiffness and strength characteristics suitable for supporting engineering structures. The estimated bearing capacity values at all locations confirm favourable foundation conditions with increasing strength at greater depths.

Overall, the study demonstrates that MASW is a reliable, economical, rapid and non-destructive geophysical technique for evaluating subsurface rock mass conditions and estimating key engineering parameters across multiple locations. The results obtained from this study provide valuable input for safe foundation design, slope stability assessment and infrastructure development at Pavagadh Hill.

REFERENCES

[1] Park CB, Miller RD, Xia J. Multichannel analysis of surface waves. Geophysics 1999; 64(3): 800-808. https://doi.org/10.1190/1.1444590

[2] Xia J, Miller RD, Park CB. Estimation of near-surface shear-wave velocity by inversion of Rayleigh waves. Geophysics 1999; 64(3): 691-700. https://doi.org/10.1190/1.1444578

[3] Miller RD, Xia J, Park CB, Ivanov J. Multichannel analysis of surface waves to map bedrock. The Leading Edge 1999; 18(12): 1392-1396. https://doi.org/10.1190/1.1438226

[4] Park CB, Miller RD, Xia J. Multichannel analysis of surface waves (MASW)—Active and passive methods. Near Surface Geophysics 2007; 5(4): 255-265.

[5] Xia J, Miller RD, Park CB, Hunter JA, Harris JB, Ivanov J. Comparing shear-wave velocity profiles from MASW and borehole measurements. Journal of Environmental & Engineering Geophysics 2002; 7(1): 1-15.

[6] Ivanov J, Miller RD, Park CB. Common-offset MASW method for near-surface investigations. Near Surface Geophysics 2006; 4(3): 173-181.

[7] Park CB, Miller RD, Xia J, Ivanov J. Passive MASW method for deep subsurface imaging. Journal of Applied Geophysics 2005; 56(4): 283-289

[8] Nazarian S, Stokoe KH. In-situ shear wave velocity using SASW method. Journal of Geotechnical Engineering 1984; 110(11): 1466-1480.

[9] Stokoe KH, Wright SG, Bay JA, Roesset JM. Characterization of geotechnical sites by SASW method. Proceedings of 3rd International Conference on Recent Advances in Geotechnical Earthquake Engineering and Soil Dynamics 1994; 1: 1-12.

[10] Pana T, Taipodia J, Philley PD. Application of active MASW study on irregular and undulated sloping terrain: A case study. International Journal of Geotechnical Engineering 2024; 18(7-10): 774-787. https://doi.org/10.1080/19386362.2024.2393402

[11] Foti S, Hollender F, Garofalo F, *et al*. Guidelines for the good practice of surface wave analysis: a product of the InterPACIFIC project. Bull Earthquake Eng 2018; 16: 2367-2420. https://doi.org/10.1007/s10518-017-0206-7

[12] Zahoor F, Rao KS, Malla SA, Tariq B, Bhat WA. Seismic Site Characterization Using MASW of Sites Along Srinagar Metro Rail Alignment, Jammu and Kashmir 2021. https://doi.org/10.1007/978-981-33-6564-3_49

[13] Pawar N, Mhaske S. Measuring shear wave velocity using MASW method to reduce cost and time required in construction projects. International Journal of Scientific Engineering and Research (IJSER) 2017; 5(7): 55-60. https://doi.org/10.70729/IJSER171627

[14] Goh TL, Rahman ZA, Hamzah U, Mohamad ET. Application of spectral analysis of surface waves (SASW) method: Rock mass characterization. Electronic Journal of Geotechnical Engineering 2011; 16: 849-858.

[15] Kausarian H. Rock Mass, Geotechnical and Rock Type Identification Using SASW and MASW Methods at Kajang Rock Quarry, Semenyih, Selangor Darul Ehsan. Journal of Ocean, Mechanical and Aerospace - Science and Engineering (JOMAse) 2015; 26(1): 7-12. https://doi.org/10.36842/jomase.v26i1.429

[16] Townsend KF, Clark MK, Zekkos D. Profiles of near-surface rock mass strength across gradients in burial, erosion, and time. Journal of Geophysical Research: Earth Surface 2021; 126(4). https://doi.org/10.1029/2020JF005694

[17] Nelliat S, *et al*. Rock Mass Characterisation and Delineation of Weak Zones in a Foundation Regime Using Integrated Geophysical Methods: A Case Study from Mangalore, India. In: Jose BT, Sahoo DK, Oommen T, Muthukkumaran K, Chandrakaran S, Santhosh Kumar TG. (Eds.) Proceedings of the Indian Geotechnical Conference 2022 Volume 5. IGC 2022. Lecture Notes in Civil Engineering, vol 483. Springer, Singapore 2024. https://doi.org/10.1007/978-981-97-3389-7_28

[18] Abdelrahman K, Saadon AB, Qaysi S. Estimating shear wave velocity and site characterization of western Riyadh City, Saudi Arabia based on multichannel analysis of surface waves. Front Earth Sci 2024; 12: 1395431. https://doi.org/10.3389/feart.2024.1395431

[19] Tiwari BD. Magmatic differentiation of the volcanics at Pavagadh, Gujarat, India. Bulletin of Volcanology 1972; 35(4): 1129-1177. https://doi.org/10.1007/BF02596869

[20] Greenough JD, Hari KR, Chatterjee AC, Santosh M. Mildly alkaline basalts from Pavagadh Hill, India: Deccan flood basalts with an asthenospheric origin. Mineralogy and Petrology 1998; 62(3): 223-245. https://doi.org/10.1007/BF01178030

[21] Furuyama K, Hari KR, Santosh M. Crystallization history of primitive Deccan basalt from Pavagadh Hill, Gujarat, Western India. Gondwana Research 2001; 4(3): 427-436. https://doi.org/10.1016/S1342-937X(05)70342-7

[22] Sheth HC, Mathew G, Pande K, Mallick S, Jena B. Cones and craters on Mount Pavagadh, Deccan Traps: Rootless cones? Proceedings of the Indian Academy of Sciences: Earth and Planetary Sciences 2004; 113(4): 831-838. https://doi.org/10.1007/BF02704041

[23] Sheth HC, Melluso L. The Mount Pavagadh volcanic suite, Deccan Traps: geochemical stratigraphy and magmatic evolution. Journal of Asian Earth Sciences 2008; 32(1): 5-21. https://doi.org/10.1016/j.jseaes.2007.10.001

[24] Singh B, Prabhakara Rao MRK, Prajapati SK, Swarnapriya C. Combined gravity and magnetic modeling over Pavagadh and Phenaimata igneous complexes, Gujarat, India: Inference on emplacement history of Deccan volcanism. Journal of Asian Earth Sciences 2014; 80: 119-133. https://doi.org/10.1016/j.jseaes.2013.11.005

[25] Sheikh JM, Sheth HC, Naik A, Keluskar T. Physical volcanology of the Pavagadh rhyolites, northern Deccan Traps: Stratigraphic, structural, and textural record of explosive and effusive eruptions. Journal of Volcanology and Geothermal Research 2020; 404: 107024. https://doi.org/10.1016/j.jvolgeores.2020.107024

[26] Dinc OS, Sonmez H, Tunusluoglu C, Kasapoglu KE. A new general empirical approach for the prediction of rock mass

strengths of soft to hard rock masses. International Journal of Rock Mechanics and Mining Sciences 2011; 48(4): 650-665. https://doi.org/10.1016/j.ijrmms.2011.03.001

[27] Vásárhelyi B, Kovács D. Empirical methods of calculating the mechanical parameters of the rock mass. Periodica Polytechnica Civil Engineering 2017; 61(1): 39-50. https://doi.org/10.3311/PPci.10095

[28] Noori KM, Alshkane YM, Rashed KA. Geotechnical and geophysical investigations of estimating rock mass properties. Iraqi Geological Journal 2023; 56(2D): 39-64. https://doi.org/10.46717/igj.56.2D.4ms-2023-10-10

[29] Hoek E, Brown ET. The Hoek-Brown failure criterion: A 2002 edition. In Rock engineering for underground mining 2002; pp. 209-213.

[30] Hoek E, Diederichs MS. Empirical estimation of rock mass modulus. International Journal of Rock Mechanics and Mining Sciences 2006; 43(2): 203-215. https://doi.org/10.1016/j.ijrmms.2005.06.005

[31] Hoek E, Brown ET. The Hoek-Brown failure criterion and GSI - 2018 edition. Journal of Rock Mechanics and Geotechnical Engineering 2019; 11(3): 445-463. https://doi.org/10.1016/j.jrmge.2018.08.001

[32] Zhang L. Evaluation of rock mass deformability using empirical methods - A review. Underground Space (China) 2017; 2(1): 1-15. https://doi.org/10.1016/j.undsp.2017.03.003

[33] Zhang L. Determination and applications of rock quality designation (RQD). Journal of Rock Mechanics and Geotechnical Engineering 2016; 8(3): 389-397. https://doi.org/10.1016/j.jrmge.2015.11.008

[34] Deere DU. Technical description of rock cores for engineering purposes. Rock Mechanics 1964; 1(1): 17-22.

[35] Bieniawski ZT. Engineering Rock Mass Classifications: A Complete Manual for Engineers and Geologists in Mining, Civil, and Petroleum Engineering. John Wiley & Sons 1989.

[36] Hoek E, Bray JW. Rock Slope Engineering. Institution of Mining and Metallurgy, London 1981. https://doi.org/10.1201/9781482267099

[37] Singh B, Goel RK. Rock Mass Classification: A Practical Approach in Civil Engineering. New Age International 2011. https://doi.org/10.1016/B978-0-12-385878-8.00006-9

https://doi.org/10.65904/3083-3590.2026.02.06